A ULFC Method for $d^4(D_{2d})$ Ions and a Study of the Spin Singlets Contributions to Zero-Field Splitting of Cr^{2+} Ions in Zinc Sulfide Crystals

Lu Cheng,[†] Kuang Xiao-Yu,[*,†,§] and Zhou Kang-Wei[‡,§,||]

Institute of Atomic and Molecular Physics, Sichuan University, Chengdu 610065, China, Department of Physics, Sichuan University, Chengdu 610065, China, International Centre for Materials Physics, Academia Sinica, Shenyang 110016, China, Chinese Center for Advanced Science and Technology (World Laboratory), P. O. Box 8730, Beijing 100080, China

Received: July 14, 2007; In Final Form: August 17, 2007

A simple theoretical method is shown to yield a detailed explanation of numerous EPR parameters for a d^4 configuration ion in tetragonal ligand field. Using the unified ligand-field-coupling (ULFC) scheme, the formulas relating the microscopic spin Hamiltonian parameters with the crystal structure parameters are derived. On the basis of the theoretical formulas, the 210×210 complete energy matrices including all the spin states are constructed within a strong field representation. By diagonalizing the complete energy matrices, the local lattice structure and Jahn−Teller energy of Cr^{2+} ions in $ZnS:Cr^{2+}$ system have been investigated. It is found that the theoretical results are in good agreement with the experimental values. Moreover, the contributions of the spin singlets to the zero-field splitting (ZFS) parameters of Cr^{2+} ions in ZnS crystals are investigated for the first time. The results indicate that the spin singlets contributions to ZFS parameter b_2^0 is negligible, but the contributions to ZFS parameters b_4^0 and b_4^4 cannot be neglected.

1. Introduction

Impurities in semiconductors have attracted a great deal of attention for many years owing to their significance for practical applications, as in photoconductors, microwave detectors, and electroluminescent devices.[1−8] Among the impurities, particular attention has been focused on the transition metal ions because they are commonly associated with deep levels within the host crystal band gap. These levels can strongly influence the electric, magnetic, and optical properties of the semiconductor because the properties of the impurity ion, such as charge, mass, and size, are different from those of the replaced host ion and the local properties in the vicinity of impurity ion, such as local compressibility and local thermal expansion coefficients, are unlike those in the host crystal. To gain more insight into the microstructure and the properties of the impurity ions in semiconductors, many studies of electron paramagnetic resonance (EPR) have been achieved.[9−11]

EPR is one of the most important and powerful techniques for the investigation of point defects in crystals. The reason is that the EPR spectra can provide highly detailed experimental information about the electronic structure, local environments, hyperfine constants, etc., of paramagnetic defects.[12−16] The EPR spectra of transition metal Cr^{2+} ions doped into ZnS have been experimentally observed by Vallin and Watkins.[11] Their experimental results give important information about the ground state of the transition metal Cr^{2+} ions and form a useful starting point for understanding the interrelationships between electronic and molecular structure of Cr^{2+} ions in the $(CrS_4)^{6-}$ coordination complex. Despite the large number of publications relating to Cr^{2+} ions in a $ZnS:Cr^{2+}$ system, as yet a comprehensive report of its zero-field splitting parameters is lacking.

Theoretically, the studies of the electronic structure of transition metal Cr^{2+} impurities in crystals have made remarkable progress in the past decades by the ^5D approximation.[17−19] However, we have not fully been able to understand the nature of transition metal Cr^{2+} ions within this approach because the contributions of spin triplet states ^3L (L = H, G, F, D, P) and the spin singlet states ^1L (L = I, G, F, D, S) have been neglected in them. To remedy these discrepancies between theory and experiments, the spin triplet states contributions to the zero-field splitting (ZFS) for a d^4 configuration ion in crystals were performed by Zhou et al.[20−22] Unfortunately, these method are still insufficient to understand the detailed information and physical origin of transition metal Cr^{2+} ions in crystals because the spin singlet states ^1L (L = I, G, F, D, S) influence the fine structure splitting of the ground states, i.e., affect the ground ZFS parameters.

It is well-known that the Hamiltonian matrix of a d^4 configuration in crystals has 210×210 dimensions for all the spin states but only 25×25 for the ^5D state and 160×160 for both ^5D and ^3L states.[23] So, to obtain more accurate ZFS, all ^{2S+1}X multiplets with S = 2, 1, and 0 should be considered. In this paper, complete energy matrices (210×210) of a d^4 configuration ion in a tetragonal ligand field are constructed and the ZFS parameters b_2^0, b_4^0, and b_4^4 of the $ZnS:Cr^{2+}$ system are investigated. By diagonalizing the complete energy matrices, the local structure distortion parameters ΔR and $\Delta\theta$ are determined.

The goal of the present study is twofold: to elucidate a microscopic origin of various ligand field parameters that are usually used empirically for the interpretation of EPR and optical absorption experiments and to provide powerful guidelines for future experimental studies aimed at pinpointing how actually Cr^{2+} enters the ZnS semiconductor. The paper is organized as

* Corresponding author. E-mail: palc@163.com.
† Institute of Atomic and Molecular Physics, Sichuan University.
‡ Department of Physics, Sichuan University.
§ International Centre for Materials Physics, Academia Sinica.
|| Chinese Center for Advanced Science and Technology (World Laboratory).

10.1021/jp075519x CCC: $37.00
Published on Web 10/05/2007

follows: In Section 2, the basic concept of the unified ligand-field-coupling (ULFC) method and the method how to construct the complete energy matrix from the standard basis are described. The spin Hamiltonian and energy levels for a d^4 configuration ion in a tetragonal ligand field are presented, and the microscopic formulas of EPR parameters for the ground state are given. In Section 3, the local structure distortion and the Jahn−Teller energy of Cr^{2+} ions in a $ZnS:Cr^{2+}$ system are investigated and the contributions of the spin singlets to ZFS are discussed. Conclusions are summarized in the final section.

2. The Unified Ligand-Field-Coupling (ULFC) Method

The applicability of the ligand field theory approach to the experimental data existing for many transition metal ions in semiconductor is well established. In the present work, the strong field scheme of the unified ligand-field-coupling (ULFC) theoretical method has been employed. ULFC method is not only a complete calculation method considering all multiplets of an d electron configuration but also a unified standardization and terse theoretical method. It uses a special standard basis for the whole d^n configuration space. This makes each basis component and each eigenstate of the corresponding energy matrix carry the information about the spin-multiplicity and the space symmetry. In addition, it also overcomes the limitations of the traditional one-by-one diagonalization methods such as the molecular orbital method, weak-field method, etc., and does not need to distinguish the ligand field strength thus can generally be applied to arbitrary transition metal complexes in principle. By this theoretical method, in this section, we will construct the spin−orbit coupling representation of the d^4 configuration space and the corresponding standard complete energy matrix of d^4 configuration ions in a tetragonal ligand field. It should be emphasized that, although the concept of standard basis was introduced by Griffith[23] for the irreducible representations of the point groups, our standard basis is defined for the whole d^4 configuration space.

The Hamiltonian of the d^4 configuration ion in a ligand field can be written as[23]

$$H = \sum_{k=1}^{+\sigma}\left\{\frac{1}{2m}\vec{P}_k^{\,2} - \frac{Ze^2}{r_k} + \zeta(r_k)\vec{l}_K\bullet\vec{S}_k + V(r_k)\right\} + \sum_{K<\lambda}^{+\sigma}\frac{e^2}{r_{k\lambda}} \quad (1)$$

where $\vec{P}_k$ is the momentum vector of the kth electron, r_k is the distance from the nucleus, m is the mass of the electron, $-e$ is the charge, $+Ze$ is the charge on the nucleus, $r_{k\lambda}$ is the distance from the kth electron to the λth electron, and $V(r_k)$ is the potential energy of the kth electron in the electrostatic field of the environment. In a cubic ligand field, it can be simplified as follows

$$H = H^0 + H^{ee}(B,C) + V_c^{A_1}(Dq) + H^{SO}(\zeta) \quad (2)$$

where H^0 is the effective center potential, $H^{ee}(B,C)$ is the electrostatic interaction between the d-electrons, $V_c^{A_1}$ is the cubic component of the crystal field, and $H^{SO}(\zeta)$ is the spin−orbit coupling energy. B and C are the Racah parameters, Dq is the ligand field intensity parameter, and ζ is the spin−orbit coupling parameter.

2.1. Standard Basis and Energy Matrix of a $d^4(O_h^*)$ System. First, we construct basis functions $|q_i,S\Gamma\Gamma'\gamma'\rangle$ for each irreducible representation Γ' (i.e., A_1, A_2, E, T_1, T_2) of the double group $O_h^*(d^4)$ with the Griffith[23] strong field functions $|q_i,S\Gamma M\gamma\rangle$ of the point group $O_h(d^4)$ according to the expression

$$|q_i,S\Gamma\Gamma'\gamma'\rangle = \sum_{M\gamma}\langle S\Gamma M\gamma|\Gamma'\gamma'\rangle|q_i,S\Gamma M\gamma\rangle \quad (3)$$

where γ' denotes different components of Γ', q_i stands for the ith strong field configuration $t_2^n(S_1\Gamma_1)e^m(S_2\Gamma_2)$ in the electrostatic matrix table of Griffith[23] for d^4 configuration. The complete strong field matrix with respect of the 210 basis functions will become a block diagonal form of 10 $\Gamma'\gamma'$ blocks. That is, the matrix splits into two 1-fold degenerated matrices A_1 (14 × 14) and A_2 (8 × 8), one 2-fold degenerated matrix E (19 × 19), two 3-fold degenerated matrices T_1 (23 × 23) and T_2 (27 × 27). Each can be looked upon as the sum of the matrices for $H^{ee}(B,C)$, $V_c^{A_1}$, and H^{so} (see Table 1). The $H^{ee}(B,C)$ component of each $\Gamma'\gamma'$ matrix is diagonal about S and Γ and thus forms a block-diagonal matrix. Of a given SΓ block, the matrix elements are just the same as the SΓ electrostatic matrix in Table A.30 of Griffith.[23]

TABLE 1: Energy Matrices of $d^4(D_{2h}^*)$

$\Gamma''\gamma''$ block	$\Gamma'\gamma'$ block	
$A_2(23\times 23)$	$T_1z(23\times 23)$	
$B_2(27\times 27)$	$T_2\zeta(23\times 23)$	
$B_1(27\times 27)$	$A_2(8\times 8)$	$E\epsilon(19\times 19)$
$A_1(33\times 33)$	$A_1(14\times 14)$	$E\theta(19\times 19)$
$Ex(50\times 50)$	$T_1x(23\times 23)$	$T_2\zeta(27\times 27)$
$Ex(50\times 50)$	$T_1y(23\times 23)$	$T_2\eta(27\times 27)$

The matrices of the cubic crystal field $V_c^{A_1}$ in each $\Gamma'\gamma'$ block will be fully diagonal in the $|q_i,S\Gamma\Gamma'\gamma'\rangle$ representation, and the diagonal elements can be obtained as follows,

$$\langle t_2^n e^m,S\Gamma\Gamma'\gamma'|V_c^{A_1}|t_2^n e^m,S\Gamma\Gamma'\gamma'\rangle = (6m-4n)Dq \quad (4)$$

The H^{so} component of a $\Gamma'\gamma'$ matrix is not diagonal, and the elements can be obtained according to the following formula,

$$H_{ij}^{so}(\Gamma',S_1\Gamma_1,S_2\Gamma_2) = \langle q_i,S_1\Gamma_1\Gamma'\gamma'|H^{so}|q_j,S_2\Gamma_2\Gamma'\gamma'\rangle = \langle q_i,S_1\Gamma_1\Gamma'\gamma'|\sum_{\gamma^*=-1}^{1}V_{\gamma^*-\gamma^*}^{1T_1}(-1)^{1+\gamma^*}|q_j,S_2\Gamma_2\Gamma'\gamma'\rangle = K'\langle q_i,S_1\Gamma_1||V^{1T_1}||q_j,S_2\Gamma_2\rangle \quad (5)$$

where K' are the transferred coefficients. The reduced matrix elements $\langle q_i,S_1\Gamma_1||V^{1T_1}||q_j,S_2\Gamma_2\rangle$ in eq 5 can be calculated with the following formula

$$\langle q_i,S_1\Gamma_1||V^{1T_1}||q_j,S_2\Gamma_2\rangle = \frac{\langle q_i,S_1\Gamma_1S_1\gamma_1|H^{so}|q_j,S_2\Gamma_2S_2\gamma_2\rangle\sqrt{(2S_1+1)\dim(\Gamma_1)}}{(-1)^{S_2-S_1-1}\langle S_2M_21\gamma|S_1M_1\rangle\langle\Gamma_2\gamma_2T_1-\gamma^*|\Gamma_1\gamma_1\rangle} \quad (6)$$

where $M_1 = S_1$, $M_2 = S_2$, and $\gamma^* = S_1 - S_2$. dim(Γ) is the dimension of Γ, and γ_1 and γ_2 can be selected arbitrarily as long as the CG coefficient $\langle\Gamma_2\gamma_2T_1-\gamma^*|\Gamma_1\gamma_1\rangle \neq 0$. From eqs 5 and 6, we can obtain all matrix elements of the spin−orbit interaction.

2.2. Standard basis and energy matrix of a $d^4(D_{2h}^*)$ system. If the octahedral ligand field has a tetragonal distortion, say, D_{2h}, the Hamiltonian can be written as

$$H' = H^0 + H^{ee}(B,C) + V_c^{A_1}(Dq) + H^{SO}(\zeta) + V^{E\theta}(\mu,\delta) \quad (7)$$

where $V^{E\theta}$ is the tetragonal component of the ligand field and μ and δ are the tetragonal distortion parameters. We can construct the $d^4(D_{2h}^*)$ basis functions for each irreducible representations Γ'' (i.e., A_1, A_2, E, B_1, B_2) of the double group D_{2h}^* (d^4) with $d^4(O_h^*)$ basis functions $|q_i,S\Gamma\Gamma'\gamma'\rangle$ by the formula below,

$$|q_i,S\Gamma\Gamma' \rightarrow \Gamma''\gamma''\rangle = \sum_{\gamma'} \langle\Gamma'\gamma'|\Gamma''\gamma''\rangle |q_i,S\Gamma\Gamma'\gamma'\rangle \quad (8)$$

where $\langle\Gamma'\gamma'|\Gamma''\gamma''\rangle$ are the coupling coefficients. The matrix of Hamiltonian (eq 7) with respect to the 210 $d^4(D_{2h}^*)$ basis functions will be a block diagonal form of six $\Gamma''\gamma''$ blocks. In each $\Gamma''\gamma''$ block, the component of $H^0 + H^{ee} + V_c^{A_1} + H^{so}$ is again a block diagonal form of $\Gamma'\gamma'$ blocks of the $d^4(O_h^*)$ matrix (see Table 1), thus only the $V^{E\theta}$ component needs to be calculated. In each $\Gamma''\gamma''$ block, the matrix elements of $V^{E\theta}$ can be at any position. Finally, each matrix element of the complete energy matrix can be expressed to be a linear combination of the Racah parameters B and C, the spin−orbit coupling coefficient ζ, and the ligand field parameters Dq, μ, and δ, which are in the following forms

$$Dq = \frac{1}{24} G_4(\tau)\left(10\cos^4\theta - \frac{20}{3}\cos^2\theta - \frac{2}{3}\right)$$

$$\mu = -\frac{8}{7} G_2(\tau)(3\cos^2\theta - 1) - G_4(\tau)\left(5\cos^4\theta - \frac{110}{21}\cos^2\theta + \frac{25}{21}\right)$$

$$\delta = -\frac{6}{7} G_2(\tau)(3\cos^2\theta - 1) + G_4(\tau)\left(5\cos^4\theta - \frac{110}{21}\cos^2\theta + \frac{25}{21}\right) \quad (9)$$

2.3. The Zero-Field Splitting Parameters. The general form of the spin Hamiltonian for a Cr^{2+} ion in a tetragonal ligand field is[24]

$$\hat{H} = \mu_B \vec{S} \bullet g \bullet \vec{B} + \frac{1}{3} b_2^0 O_2^0 + \frac{1}{60}(b_4^0 O_4^0 + b_4^4 O_4^4) \quad (10)$$

where the first term corresponds to the Zeeman interaction, and the following terms represent the zero-field splitting effect. μ_B is the Bohr magneton, $\vec{B}$ is the magnetic field, g is the splitting factor, $\vec{S}$ is the spin angular momentum operator, b_k^q are the EPR zero-field splitting parameters, and O_k^q are the standard Stevens spin operators.[25] It is noteworthy to mention that the parametersb_k^q are related to the EPR parameters a, D, and F. a is the cubic field splitting parameter, D and F correspond to axial component of the second-order and the fourth-order, respectively. The relationships are given by

$$a = \frac{2}{5} b_4^4, \qquad D = b_2^0, \qquad F = 3b_4^0 - \frac{3}{5} b_4^4 \quad (11)$$

From the spin Hamiltonian (eq 10), we can get the expressions of the splitting energy levels E_i in the ground state for a zero magnetic field, which are expressed as follows

$$E_1 = 2b_2^0 + \frac{1}{5}b_4^0 + \frac{1}{5}b_4^4, \qquad E_2 = 2b_2^0 + \frac{1}{5}b_4^0 - \frac{1}{5}b_4^4,$$

$$E_3 = -b_2^0 - \frac{4}{5}b_4^0, \qquad E_4 = -2b_2^0 + \frac{6}{5}b_4^0 \quad (12)$$

The corresponding matrix elements are presented in Table 2. Using eq 12, we can easily obtain that

$$b_2^0 = \frac{1}{7}(E_1 + E_2 - E_3 - E_4),$$

$$b_4^0 = \frac{1}{14}(E_1 + E_2 - 8E_3 + 6E_4),$$

$$b_4^4 = \frac{5}{2}(E_1 - E_2) \quad (13)$$

The values of E_i can be obtained by a comparison with the eigenvalues of the $d^4(D_{2h}^*)$ matrix that correspond to the orbitally nondegenerated ground state.

3. Calculation for Cr^{2+} Ions in the ZnS:Cr^{2+} Complex System

3.1. The Local Structure Distortion of Cr^{2+} Ions in ZnS. ZnS has a cubic zinc-blende structure at low temperature but a hexagonal wurzite structure at high temperatures. The EPR study of Cr^{2+} ions in ZnS crystals has been done by Vallin and Watkins at 4.2 K.[11] The Cr^{2+} ion appears as a substitutional impurity at the cation site, surrounded by four S anions in the tetrahedral coordination. The local lattice structure around the Cr^{2+} ion displays a tetragonal distortion.[26] The tetragonal distortion can be described by employing two parameters, ΔR and $\Delta\theta$, as shown in Figure 1. We used the following relationship to evaluate the bond length R and bond angle θ for Cr^{2+} ions in ZnS.

$$R = R_0 + \Delta R, \qquad \theta = \theta_0 + \Delta\theta \quad (14)$$

where $R_0 = 2.341$ Å and $\theta_0 = 54.7356°$. To decrease the number of adjustable parameters and reflect the covalency effects, we use the Curie et al.'s covalent theory and take an average covalence factor N to determine the optical parameters as following[27]

$$B = N^4 B_0, \qquad C = N^4 C_0, \qquad \zeta = N^2 \zeta_0 \quad (15)$$

where B_0, C_0, and ζ_0 are the free-ion parameters for Cr^{2+} ion and can be determined from the spectra of the free Cr^{2+} ion.[28] The comparisons between the calculation and experiment are shown in Tables 3 and 4.

According to the Van Vleck approximation and eq 9, we may obtain the following relations[29]

$$G_2(\tau) = \frac{-eq_\tau\langle r^2\rangle}{R^3} = \frac{A_2}{R^3}, \qquad G_4(\tau) = \frac{-eq_\tau\langle r^4\rangle}{R^5} = \frac{A_4}{R^5} \quad (16)$$

where $A_2 = -eq_\tau\langle r^2\rangle$, $A_4 = -eq_\tau\langle r^4\rangle$, and $A_2/A_4 = \langle r^2\rangle/\langle r^4\rangle$. The ratio of $\langle r^2\rangle/\langle r^4\rangle = 0.122478$ is obtained from the radial wave function of Cr^{2+} ion.[26] For A_4, as a constant for the $(CrS_4)^{6-}$ tetrahedron, its value can be determined from the optical absorption spectra and the Cr−S band length of the CrS crystal.[30−31] Thus, from the optical spectra of CrS, we obtain $A_4 = 41.2636$ au and $A_2 = 5.0361$ au for Cr^{2+} ions in the $(CrS_4)^{6-}$ coordination complex. For Cr^{2+} ions in ZnS:Cr^{2+} system, by diagonalizing the complete energy matrices, the ground-state ZFS can be calculated with use of distortion

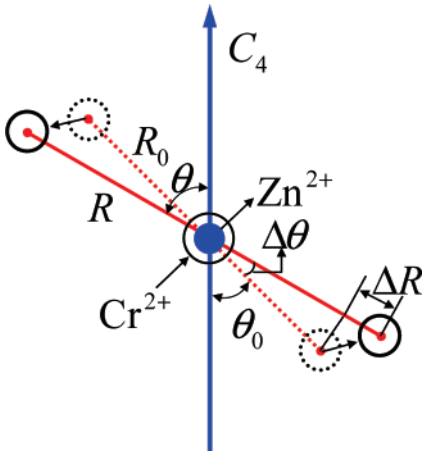

Figure 1. Local structure distortion for Cr^{2+} ions in ZnS:Cr^{2+} system. ΔR and $\Delta\theta$ represent the structure distortion.

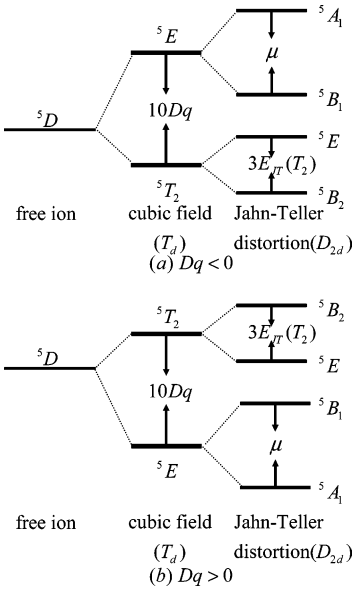

Figure 2. Energy levels of Cr^{2+} ions in a tetragonal symmetry (D_{2d}), as predicted by ligand field theory in presence of a static Jahn−Teller effect.

TABLE 2: Spin Hamiltonian Matrix

S,M_S	2,2	2,1	2,0	2,−1	2,−2
2,2	$2b_2^0 + {}^1/_5 b_4^0$	0	0	0	${}^1/_5 b_4^4$
2,1	0	$-b_2^0 - {}^4/_5 b_4^0$	0	0	0
2,0	0	0	$-2b_2^0 + {}^6/_5 b_4^0$	0	0
2,−1	0	0	0	$-b_2^0 - {}^4/_5 b_4^0$	0
2,−2	${}^1/_5 b_4^4$	0	0	0	$2b_2^0 + {}^1/_5 b_4^0$

parameters ΔR and $\Delta\theta$ and the covalence factor N. The comparisons between the theoretical values and experimental findings are shown in Table 5.

It can be seen from Table 5 that the distortion parameters $\Delta R = 0.048$ Å and $\Delta\theta = 1.554°$ can provide a satisfactory explanation for the experimental ZFS parameters b_2^0, b_4^0, and b_4^4. $\Delta R > 0$ indicates that the local lattice structure of ZnS:Cr^{2+} system has an expansion distortion. The expansion distortion may be partly because the Cr^{2+} ion has an obviously larger ionic radius ($r_{Cr^{2+}} = 0.89$ Å) than that of the Zn^{2+} ion ($r_{Zn^{2+}} = 0.74$ Å) and the Cr^{2+} ion will push the S ligand to move upward and downward, respectively, and this will lead to a local elongate effect of the sublattice. From the calculation, the local lattice structure parameters $R = 2.389$ Å and $\Delta\theta = 56.2896°$ for Cr^{2+} ions in ZnS:Cr^{2+} system have been determined.

TABLE 3: Spectra of Free Cr^{2+} Ion

		energy levels (cm^{-1})	
term	J	theoretical value	experimental value[a]
^5D	0	0.00	0.00
	1	62.49	62.22
	2	185.31	183.16
	3	364.72	356.55
	4	596.13	576.08
$^3P_2$	0	16701.48	16771.36
	1	17149.99	17168.56
	2	17800.11	17851.18
^3H	4	17216.37	17273.70
	5	17389.25	17396.92
	6	17508.91	17530.65
$^3F_2$	2	18421.41	18451.84
	3	18471.02	18511.18
	4	18550.53	18583.39
^3G	3	20775.68	20703.64
	4	20937.36	20852.95
	5	21070.23	20996.04
$^1G_2$	4	25201.22	25138.87
^3D	3	25770.36	25726.44
	2	25826.55	25780.94
	1	25879.84	25848.31
^1I	6	26036.71	26014.89
$^1S_2$	0	27467.10	27372.32
$^1D_2$	2	32217.58	32151.99
^1F	3	37109.61	37005.16
$^3F_1$	4	43301.15	43286.71
	2	43352.90	43304.53
	3	43389.56	43322.17
$^3P_1$	2	43479.24	43441.99
	1	44013.43	43916.59
	0	44190.47	44141.36
$^1G_1$	4	49818.14	49768.65
$^1D_1$	2	65848.03	65763.21

[a] Reference 28.

TABLE 4: Free-Ion Parameters B_0, C_0, and ζ_0 for $d^4(d^6)$ Ion, in Units of cm^{-1}

ions	B_0	C_0	ζ_0
Cr^{2+}	843.7[a]	3486.6[a]	236.1[a]
Cr^{2+}	830[b]	3430[b]	230[b]
Cr^{2+}	870.6[c]	3135.7[c]	232[c]
Mn^{3+}	1140[b]	3675[b]	352[b]
Fe^{2+}	1058[b]	3901[b]	410[b]

[a] The present work. [b] Reference 23. [c] Reference 26.

3.2. The Jahn−Teller Energy of Cr^{2+} Ions in ZnS. When Cr^{2+} ions are doped into the ZnS, the system undergoes a Jahn−Teller distortion, effecting a change in the Cr^{2+} ion site symmetry from the tetrahedral symmetry (T_d) to tetragonal symmetry (D_{2d}).[11,32−34] As a result of the Jahn−Teller interaction, the $^5T_2$ state is split into a $^5B_2$ ground state and a ^5E state elevated by $3E_{JT}(T_2)$ (E_{JT} is the Jahn−Teller energy), whereas the excited $^5E(T_d)$ state is split into $^5B_1$ and $^5A_1$ components (see Figure 2). For Cr^{2+} ions in ZnS:Cr^{2+} system, the experiment shows that the Jahn−Teller energy E_{JT} is about 306.3−378 cm^{-1}.[32−34] Substituting the optical parameters $N = 0.974$ and the structure distortion parameters $\Delta R = 0.048$ Å and $\Delta\theta = 1.554°$ into the complete energy matrices, we can obtain the Jahn−Teller energy $E_{JT} = 343.42$ cm^{-1}, which agrees well with the experimental results. By diagonalizing the complete energy

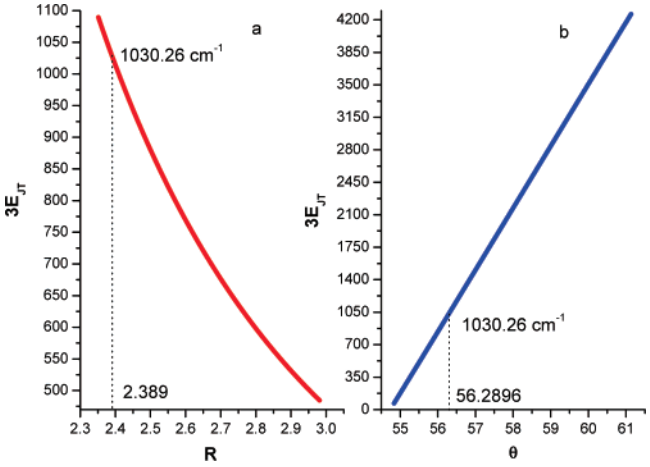

Figure 3. Jahn−Teller energy E_{JT} for Cr^{2+} ions in the ZnS:Cr^{2+} system as a function of the local lattice structure parameters R and θ. (a) $N = 0.974$, $\theta = 56.2896°$; (b) $N = 0.974$, $R = 2.389$ Å

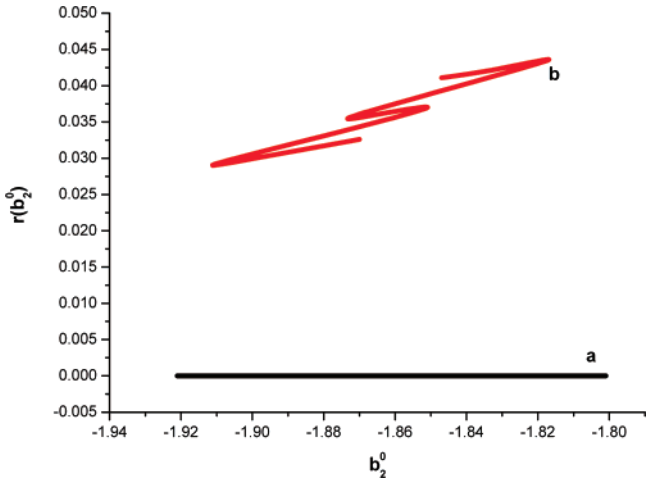

Figure 4. Spin singlets and spin triplets contributions to the second-order zero-field splitting parameter b_2^0 of the ZnS:Cr^{2+} system. (a) Neglecting the spin singlets; (b) neglecting the spin singlets and the spin triplets.

TABLE 5: Zero-Field Splitting Parameters b_2^0, b_4^0, and b_4^4 for Cr^{2+} Ions in ZnS:Cr^{2+} System as a Function of the Three Parameters ΔR, $\Delta\theta$, and N[a]

N	ΔR (Å)	$\Delta\theta$ (deg)	b_2^0	b_4^0	b_4^4	ΔE_{21}	ΔE_{31}	ΔE_{41}
0.984	0.040	1.550	−1.870	0.0441	0.4950	0.198	5.664	7.622
0.984	0.048	1.554	−1.906	0.0455	0.5075	0.203	5.774	7.771
0.984	0.050	1.560	−1.921	0.0455	0.5075	0.203	5.819	7.831
0.974	0.040	1.550	−1.834	0.0415	0.4725	0.189	5.555	7.472
0.974	**0.048**	**1.554**	**−1.868**	**0.0428**	**0.4825**	**0.193**	**5.659**	**7.613**
0.974	0.050	1.560	−1.883	0.0425	0.4825	0.193	5.703	7.671
0.964	0.040	1.550	−1.801	0.0391	0.4500	0.180	5.453	7.332
0.964	0.048	1.554	−1.833	0.0403	0.4600	0.184	5.552	7.466
0.964	0.050	1.560	−1.847	0.0404	0.4600	0.184	5.593	7.521
expt[a]			**−1.860**	**0.0498**	**0.483**	**0.193**	**5.627**	**7.586**

[a] Where zero-field splitting parameters b_2^0, b_4^0, b_4^4, and energy levels $\Delta E_{21} = E_2 - E_1$, $\Delta E_{31} = E_3 - E_1$, $\Delta E_{41} = E_4 - E_1$ are in units of cm^{-1}. [b] Reference 11.

matrices, we can find that the Jahn−Teller energy E_{JT} is strongly associated with the local lattice structure parameters R and θ. The relationships of the structure parameters R and θ vs E_{JT} are shown in Figure 3. From Figure 3, we can see that the Jahn−Teller energy will reduce when the bond length R increase, whereas the Jahn−Teller energy will increase when the bond angle θ increase and the change of the Jahn−Teller energy is almost linear.

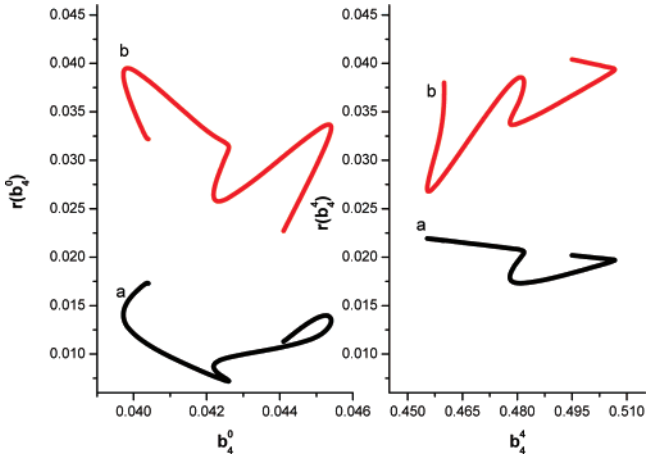

Figure 5. Spin singlets and spin triplets contributions to the fourth-order zero-field splitting parameters b_4^0 and b_4^4 of the ZnS:Cr^{2+} system. (a) Neglecting the spin singlets; (b) neglecting the spin singlets and the spin triplets.

TABLE 6: Zero-Field Splitting Parameters of ZnS:Cr^{2+} System as a Function of ΔR, $\Delta\theta$, and N, Where b_2^0, b_4^0, b_4^4 are in Units of cm^{-1}

N	R (Å)	θ (deg)	$(b_2^0)^a$	$(b_4^0)^a$	$(b_4^4)^a$	$(b_2^0)^b$	$(b_4^0)^b$	$(b_4^4)^b$
0.984	2.381	56.2856	−1.870	0.0436	0.5050	−1.809	0.0431	0.5150
0.984	2.389	56.2896	−1.906	0.0448	0.5175	−1.850	0.0440	0.5275
0.984	2.391	56.2956	−1.921	0.0450	0.5175	−1.867	0.0439	0.5275
0.974	2.381	56.2856	−1.834	0.0411	0.4800	−1.763	0.0406	0.4875
0.974	2.389	56.2896	−1.869	0.0425	0.4925	−1.802	0.0414	0.5000
0.974	2.391	56.2956	−1.883	0.0422	0.4925	−1.818	0.0412	0.5025
0.964	2.381	56.2856	−1.801	0.0386	0.4600	−1.719	0.0374	0.4600
0.964	2.389	56.2896	−1.833	0.0396	0.4700	−1.756	0.0390	0.4750
0.964	2.391	56.2956	−1.847	0.0397	0.4700	−1.771	0.0391	0.4775

[a] Neglecting the spin singlets. [b] Neglecting the spin singlets and the spin triplets.

TABLE 7: Spin Singlets and Spin Triplets Contributions to the Zero-Field Splitting Parameters b_2^0, b_4^0, b_4^4 of ZnS:Cr^{2+} System

N	R (Å)	θ (deg)	$(r_{b_2^0})^a$	$(r_{b_2^0})^b$	$(r_{b_4^0})^a$	$(r_{b_4^0})^b$	$(r_{b_4^4})^a$	$(r_{b_4^4})^b$
0.984	2.381	56.2856	0	0.0326	0.0113	0.0227	0.0202	0.0404
0.984	2.389	56.2896	0	0.0294	0.0154	0.0330	0.0197	0.0394
0.984	2.391	56.2956	0	0.0281	0.0110	0.0352	0.0197	0.0394
0.974	2.381	56.2856	0	0.0387	0.0096	0.0217	0.0159	0.0317
0.974	2.389	56.2896	0	0.0358	0.0070	0.0327	0.0207	0.0363
0.974	2.391	56.2956	0	0.0345	0.0071	0.0306	0.0207	0.0415
0.964	2.381	56.2856	0	0.0455	0.0128	0.0435	0.0222	0.0222
0.964	2.389	56.2896	0	0.0420	0.0174	0.0323	0.0217	0.0326
0.964	2.391	56.2956	0	0.0411	0.0173	0.0322	0.0217	0.0380

[a] Neglecting the spin singlets. [b] Neglecting the spin singlets and the spin triplets.

3.3. The Spin Singlets Contributions to ZFS of Cr^{2+} Ions in ZnS. For further studying of the spin singlets contributions to the ZFS parameters, we use the following relationship to show the spin singlets contributions to the ZFS of Cr^{2+} ions in ZnS

$$r_{b_{2i}^0} = \left|\frac{b_2^0 - b_{2i}^0}{b_2^0}\right|, \quad r_{b_{4i}^0} = \left|\frac{b_4^0 - b_{4i}^0}{b_4^0}\right|, \quad r_{b_{4i}^4} = \left|\frac{b_4^4 - b_{4i}^4}{b_4^4}\right| \qquad (17)$$

By diagonalizing the complete energy matrices, we can obtain the theoretical results of the spin singlets contributions to the ZFS parameters. The detailed results are presented in Figures

4−5. It is obvious that the larger the ratio r, the larger are the contributions to the ZFS parameters. From Figures 4−5, we can see that the spin singlets contributions to the second-order ZFS parameter b_2^0 are negligible, but the contributions to the fourth-order ZFS parameters b_4^0 and b_4^4 cannot be neglected and the values r for b_4^4 are more than that for b_4^0. It can be also seen from Figures 4−5 that the values r for ^5D approximation is more than 0.30 for second-order ZFS parameter b_2^0 and 0.25 for fourth-order ZFS parameters b_4^0 and b_4^4. This means that the ^5D approximation method is imperfect. A part of the quantitative calculation results are listed in Tables 6 and 7.

4. Conclusion

By using the unified ligand-field-coupling (ULFC) method, we establish the interrelationships between electronic and molecular structure and study the local molecular structure of the $(CrS_4)^{6-}$ coordination complex. From the above studies, we have the following conclusions:

(i) The zero-field splitting parameters b_2^0, b_4^0, and b_4^4 of Cr^{2+} ions in ZnS:Cr^{2+} system have been studied by the 210 × 210 complete energy matrices for a d^4 configuration ion in tetragonal ligand field. By diagonalizing the complete energy matrices, the local structure distortion parameters $\Delta R = 0.048$ Å and $\Delta\theta = 1.554°$ are determined. The results show that the local lattice structure of $(CrS_4)^{6-}$ coordination complex for Cr^{2+} ions in a ZnS:Cr^{2+} system has an expansion distortion. This distortion may be partly because of that the Cr^{2+} ion has an obviously larger ionic radius ($r_{Cr^{2+}} = 0.89$ Å) than that of Zn^{2+} ion ($r_{Zn^{2+}} = 0.74$ Å). Of course, careful experimental investigations, especially ENDOR experiments, are required in order to clarify the local lattice structure around the Cr^{2+} ions in ZnS:Cr^{2+} system in detail.

(ii) The Jahn−Teller energy $E_{JT} = 343.42$ cm^{-1} has been derived, and the theoretical values are found to be in good agreement with the experimental finds.

(iii) The spin singlets contributions to the zero-field splitting parameters of Cr^{2+} ions in ZnS:Cr^{2+} system are investigated for the first time. From our calculation, we find that the spin singlets contributions to the zero-field splitting parameters b_4^0 and b_4^4 are so large that by neglecting these contributions one cannot obtain accurate values of b_4^0 and b_4^4. Thus, many previous works[17−22] neglecting the spin singlets should be reconsidered to obtain more accurate fourth-order ZFS parameters b_4^0 and b_4^4.

Acknowledgment. We express our gratitude to Dr. Du He for many helpful discussions. This work was supported by the National Natural Science Foundation (nos. 10774103, 10374068) and the Doctoral Education Fund of Education Ministry (no. 20050610011) of China.

References and Notes

(1) Gonzalez Beermann, P. A.; McGarvey, B. R.; Muralidharan, S.; Sung, R. C. W. *Chem. Mater.* **2004**, *16*, 915.
(2) Quan, Z.; Wang, Z.; Yang, P.; Lin, J.; Fang, J. *Inorg. Chem.* **2007**, *46*, 1354.
(3) Chung, J. H.; Ah, C. S.; Jang, D. J. *J. Phys. Chem. B* **2001**, *105*, 4128.
(4) Bol, A. A.; Meijerink, A. *J. Phys. Chem. B* **2001**, *105*, 10197.
(5) Bol, A. A.; Meijerink, A. *J. Phys. Chem. B* **2001**, *105*, 10203.
(6) Su, F. H.; Fang, Z. L.; Ma, B. S.; Ding, K.; Li, G. H.; Chen, W. *J. Phys. Chem. B* **2003**, *107*, 6991.
(7) Haranath, D.; Chander, H.; Bhalla, N.; Sharma, P.; Sood, K. N. *Appl. Phys. Lett.* **2005**, *86*, 201904.
(8) Do, Y. R.; Kim, Y. C.; Cho, S. H.; Zang, D. S.; Huh, Y. D.; Yun, S. J. *Appl. Phys. Lett.* **2004**, *84*, 1377.
(9) Lu, X.; Tsoi, S.; Miotkowski, I.; Rodriguez, S.; Ramdas, A. K.; Alawadhi, H. *Phys. Rev. B* **2007**, *75*, 155206.
(10) Malguth, E.; Hoffmann, A.; Gehlhoff, W.; Gelhausen, O.; Phillips, M. R.; Xu, X. *Phys. Rev. B* **2006**, *74*, 165202.
(11) Vallin, J. T.; Warkins, G. D. *Phys. Rev. B* **1974**, *9*, 2051.
(12) Renault, J. P.; Verchere-Beaur, C.; Morgenstern-Badarau, I.; Yamakura, F.; Gerloch, M. *Inorg. Chem.* **2000**, *39*, 2666.
(13) Harmer, J.; Van Doorslaer, S.; Gromov, I.; Broring, M.; Jeschke, G.; Schweiger, A. *J. Phys. Chem. B* **2002**, *106*, 2801.
(14) Freysoldt, C.; Poppl, A.; Reinhold, J. *J. Phys. Chem. A* **2004**, *108*, 1582.
(15) Doorslaer, S. V.; Bachmann, R.; Schweiger, A. *J. Phys. Chem. A* **1999**, *103*, 5446.
(16) Pietrzyk, P.; Piskorz, W.; Sojka, Z.; Broclawik, E. *J. Phys. Chem. B* **2003**, *107*, 6105.
(17) Rudowicz, C.; Zhou, Y. Y.; Yu, W. L. *J. Phys. Chem. Solids* **1992**, *53*, 1227.
(18) Rudowicz, C.; Zhou, Y. Y. *J. Magn. Magn. Mater.* **1992**, *111*, 153.
(19) Rudowicz, C.; Du, L. M.; Yeung, Y. Y.; Zhou, Y. Y. *Physica B* **1993**, *191*, 323.
(20) Zhou, Y. Y.; Li, C. L. *Phys. Rev. B* **1993**, *48*, 16489.
(21) Zhou, Y. Y. *Phys. Rev. B* **1994**, *50*, 7161.
(22) Li, F. Z.; Li, D. H.; Zhou, Y. Y. *Physica B* **1998**, *252*, 167.
(23) Griffith, J. S. *The Theory of Transition-Metal Ions*; Cambridge University Press: Cambridge, U.K., 1961.
(24) Abragam, A.; Bleaney, B. *Electron Paramagnetic Resonance of Transition Ions*; Clarendon Press: Oxford, U.K., 1970.
(25) Stevens, K. W. H. *Proc. Phys. Soc., London, Sect. A* **1952**, *65*, 209.
(26) Zhao, M. G.; Xie, L. H. *Mater. Sci. Eng., B* **2000**, *75*, 72.
(27) Curie, D.; Barthon, C.; Canny, B. *J. Chem. Phys.* **1974**, *61*, 3048.
(28) Jack, S.; Charles, C. *J. Phys. Chem. Ref. Data* **1977**, *6*, 317.
(29) Vleck, J. H. V. *Phys. Rev.* **1932**, *41*, 208.
(30) Shi, Q.; Ran, Q.; Tam, W. S.; Leung, J. W. H.; Cheung, A. S. C. *Chem. Phys. Lett.* **2001**, *339*, 154.
(31) Vore, T. C. De. Ph.D. Thesis, Iowa State University, Ames, IA, 1975.
(32) Kaminska, M.; Baranowski, J. M.; Uba, S. M.; Vallint, J. T. *J. Phys. C: Solid State Phys.* **1979**, *12*, 2197.
(33) Boonman, M. E.; Mac, W.; Twardowski, A.; Wittlin, A.; Bentum, P. J. V.; Maan, J. C.; Demianiuk, M. *Phys. Rev. B* **2000**, *61*, 5358.
(34) Bevilacqua, G.; Martinelli, L.; Vogel, E. E.; Mualin, O. *Phys. Rev. B* **2004**, *70*, 075206.